MPE — Volume 2, pp. 143-163
Reprints available directly from the publisher
Photocopying permitted by license only

HYBRID PROBABILITIC AND CONVEX MODELING OF EXCITATION AND RESPONSE OF PERIODIC STRUCTURES

L. P. ZHU and I. ELISHAKOFF

Department of Mechanical Engineering, Florida Atlantic University, Boca Raton, Florida 33431-0991

Accepted for publication by Dr. Gary Anderson

(Received March 8, 1993)

In this paper, a periodic finite-span beam subjected to the stochastic acoustic pressure with *bounded* parameters is investigated. Uncertainty parameters exist in this acoustic excitation due to the deviation or imperfection. First, a finite-span beams subjected to the random acoustic pressure field are studied, the exact analytic forms of the cross-spectral density of both the transverse displacement and the bending moment responses of the structure are formulated. The combined probabilistic and convex modeling of acoustic excitation appears to be most suitable, since there is an insufficient information available on the acoustic excitation parameters, to justify the totally probabilitic analysis. Specifically, we postulate that the uncertainty parameters in the acoustic loading belong to a bounded, convex set. In the special case when this convex set is an ellipsoid, closed form solutions are obtained for the most and least favorable mean square responses of both the transverse displacement and bending moment of the structure. Several finite-span beams are exemplified to gain insight into proposal methodology.

KEYWORDS: *Probabilistic analysis; convex modeling; multi-span structures*

1. INTRODUCTION

The model of a periodic multi-span beam with elastic supports is often utilized in engineering. For example, such a model is a reasonable approximation for a plate-like structure with parallel, regularly spaced stiffeners. Other practical examples of such periodic structures include an airplane fuselage structure consisting of a uniform shell reinforced with periodically arranged stiffeners, and an oil pipe line or a long bridge lying on periodic supports, etc.

There are several approaches dealing with the free vibration of multi-span beam [1–5], but only several studies have been conducted on forced vibration under either deterministic or random excitation. The usual normal mode formulation does not lead to practical results in this case, since it is almost impossible to calculate the normal modes of structures with a large number of spans due to close proximity of natural frequencies in each frequency band. However, if the structural configuration is spatially periodic, then the analysis can be greatly simplified. Two alternative methods are available for such a spatially periodic multi-span beam: the transfer matrix technique [6] and the wave-propagation approach [5,7–9]. However, numerical difficulty in transfer matrix technique may still arise when the number of periodic units in a structure is large. In the framework of wave propagation, *non-harmonic* waves have to be decomposed into an infinite number

of *harmonic* components in order to carry out the analysis of the forced vibration. In the actual calculation, however, the infinite sum has to be truncated, and a large number of linear equations has to be solved numerically to determine the unknown coefficients. Recently, the unavoidable disorders (i.e. diviation from the perfect periodicity) attracted several investigators. For the review of these works and the effect of mode localization, readers may consult the extensive review of Li and Benaroya [10]. The mode localization in eigenvalue problems was dealt *inter alia* by Ariaratnam and Xie [11], Hodges and Woodhouse [12], Pierre and Dowell [13], Elishakoff, Li, and Starnes [14], and others.

In this paper, first, a finite-span beams subjected to the random acoustic pressure field are studied, the exact analytic forms of the cross-spectral density of both the transverse displacement and the bending moment responses of the structure are formulated by utilizing the exact normal modes of a finite-span beam proposed in paper [15]. Several examples are selected for illustration, namely, beams with different span numbers which typify many structural systems often found in engineering.

In a traditional random vibration analysis, the probabilistic parameters of the random loading are assumed to be precisely known. This crucial conjecture is then dispensed within this paper. Specifically, we postulate that the loading probabilistic parameters belong to a bounded, convex set. A convex model is a set of functions. Each member function represents a possible realization of an uncertain event. In this paper our convex models represent uncertain space-wise and time-wise varying excitation vectors. The set of functions represents the uncertainty in the actual realization. Many different convex models are available, and one selects among them according to the type of information which characterizes the uncertainty. In the special case when this convex set is an ellipsoid, closed form solutions are given for the upper and lower bounds of the mean-square displacement of the structure. This combined probabilistic and convex-theoretic approach toward uncertainty in loading statistical parameters was first proposed and developed by Elishakoff and Columbi [16, 17]. Here we will apply this approach to establish a convex model for the acoustic pressure and use this convex model to estimate the least favorable stochastic responses of the multi-span beams.

2. RANDOM VIBRATION OF THE SYSTEM

2.1. Basic Equations

Consider a multi-span beam whose motion is governed by the following differential equation

$$EI \frac{\partial^4 w(x,t)}{\partial x^4} + c \frac{\partial w(x,t)}{\partial t} + \rho A \frac{\partial^2 w(x,t)}{\partial t^2} = p(x,t) \tag{1}$$

where EI = the bending stiffness of beam, c = viscous damping coefficient, ρA = mass per length of the beam, and $p(x, t)$ = the stochastic acoustic pressure.

We assume that the acoustic pressure field is a weakly stationary random process in time. The calculation of the cross-spectral density of the response at a given location on the linear system requires that the cross-spectral density of the excitation field be known.

The following model of the cross-spectral density $\Phi_{pp}(\rho_1, \rho_2; \omega)$ for acoustic loading was chosen in the this study

$$\Phi_{pp}(\rho_1, \rho_2; \omega) = \Phi_0(\omega)\, \psi(\Delta\rho, \omega)\, e^{-i\gamma(\omega)\Delta\rho}, \quad \Delta\rho = \rho_1 - \rho_2 \tag{2}$$

where $S_p(\omega)$ is the spectral density when $\rho_1 = \rho_2$, $\alpha(\omega)$ and $\gamma(\omega)$ are the decay and phase functions, respectively, which are given by Eqs. (B.1), (B.2) and (B.3) in Appendix B.

Let the dynamic behavior of the system be characterized by the frequency response function $H(r; \rho; \omega)$ which will be derived later. Hence, the cross-spectral density of the response at r_1 and r_2 is given:

$$\Phi_{00}(r_1, r_2, \omega) = \int_R \int_R \Phi_{pp}(\rho_1, \rho_2; \omega)\, H_0(r_1, \rho_1; \omega)\, H_0^*(r_2, \rho_2; \omega)\, d\rho_1\, d\rho_2 \tag{3}$$

where the subscript *0* indicates a certain response (or output) variable, $\Phi_{pp}(\rho_1, \rho_2; \omega)$ = cross spectral density of the pressure intensities at ρ_1 and ρ_2, respectively. Each integration in Eq. (3) is over the domain R of the structure. The cross spectral density $\Phi_{pp}(\rho_1, \rho_2, \omega)$ reduces to the spectral density in a single location for $\rho_1 = \rho_2 = \rho$.

2.2 Cross-Spectral Density of Responses

For an N-span beam, it is more convenient to use local coordinates rather than global coordinate systems. The global and local coordinates are related as follows

$$r_j = (\xi_j + \beta_j - 1)\, L; \quad \rho_j = (\xi_j' + \beta_j' - 1)\, L$$

$$0 \le \xi_j, \xi_j' \le 1$$

$$\beta_j, \beta_j' = 1,2,\cdots, N; \quad j = 1,2. \tag{4}$$

where r_j is the response location, ρ_j is the location where the force is imposed, β and β' are the serial number of beam's span. Thus, the cross-spectral density of displacement response in Eq. (3) for N-span beam reduces to the following expression in terms of the local coordinate system:

$$\Phi_{DD}(\beta_1, \xi_1; \beta_2, \xi_2; \omega) = B^2 L^2 \sum_{\beta_1'=1}^{N} \sum_{\beta_2'=1}^{N} \int_0^1 \int_0^1 \Phi_{pp}(\xi_1' - \xi_2' + \beta_1' - \beta_2'; \omega)$$

$$\times\ H_D(\beta_1, \xi_1; \beta_1', \xi_1'; \omega)\, H_D^*(\beta_2, \xi_2; \beta_2', \xi_2'; \omega)\ d\xi_1'\, d\xi_2' \tag{5}$$

where B is the width of the beam, an asterisk indicates the complex conjugate.

Similarly, the cross-spectral density of response for bending moment can be obtained from Eq. (5) with replacement of H_D by H_M as follows:

$$\Phi_{MM}(\beta_1, \xi_1; \beta_2, \xi_2; \omega) = B^2 L^2 \sum_{\beta_1=1}^{N} \sum_{\beta_2=1}^{N} \int_0^1 \int_0^1 \Phi_{pp}(\xi_1' - \xi_2' + \beta_1' - \beta_2'; \omega)$$

$$\times H_M(\beta_1, \xi_1; \beta_1', \xi_1'; \omega) H_M^*(\beta_2, \xi_2; \beta_2', \xi_2'; \omega) d\xi_1' d\xi_2' \tag{6}$$

where H_M can be obtained from H_D

$$H_M(\xi, \beta, \xi', \beta'; \omega) = EIL^{-2} \frac{\partial^2 H_D(\xi, \beta, \xi', \beta', \omega)}{\partial \xi^2} \tag{7}$$

In order to derive the functions H_D and H_M, let us assume that the multi-span beam is excited by a harmonic point loading imposed at ξ' on β'th span of the beam, i.e.

$$p_\beta(\xi, t) = \delta_{\beta\beta'} \delta(\xi - \xi') e^{i\omega t} \tag{8}$$

where $\delta_{\beta\beta'}$ = Kronecker's delta and $\delta(\xi - \xi')$ = Dirac's delta function. The response of the system at ξ on βth span is sought in the form

$$w_\beta(\xi, t) = H_D(\beta, \xi; \beta', \xi'; \omega) e^{i\omega t} \tag{9}$$

Substitution of Eqs. (8) and (9) into Eq. (1) yields

$$EIL^{-4} H_D^{(4)} + (ic\omega - \rho A\omega^2) H_D = \delta_{\beta\beta'} \delta(\xi - \xi') \tag{10}$$

Here, H_D is expended in series of the mode shapes of multi-span beam

$$H_D(\beta, \xi; \beta', \xi'; \omega) = \sum_{j=1}^{\infty} c_j W_{\beta,j}(\xi) \tag{11}$$

where $W_{\beta j}(\xi)$ = mode shape for an N-span beam derived in Ref. [11] as follows:

$$W_{\beta,j}(\xi) = \Lambda_j \{W_\beta(\xi, \mu_j, \lambda_j) + \Gamma_j W_\beta(\xi, -\mu_j, \lambda_j)\} \tag{12}$$

Here, $W_\beta(\xi, \mu_j, \lambda_j)$ is mode shape of infinite-span beam, Λ_j and Γ_j are the constants determined by boundary conditions at the extreme ends of N-span beam. They are listed in Appendix A for the completeness. Substituting Eq. (11) into Eq. (10) and applying the orthogonality conditions of normal mode for N-span beam, we obtain the expressions for c_j as follows

$$c_j = \frac{1}{\gamma_j^2} H(\lambda_j, \lambda_f) W_{\beta',j}(\xi') \tag{13}$$

where γ_j^2 and $H(\cdot)$ are the norm of mode shapes and the frequency response function, respectively, which are also given in Appendix A. Hence, the cross-spectral densities of

response for both transverse displacement and bending moment may be rewritten from Eqs. (5) and (6) as follows:

$$\Phi_{DD}(\beta_1, \xi_1; \beta_2, \xi_2; \omega) = (B\,L)^2\; S_p(\omega) \sum_{j_1=1}^{\infty} \sum_{j_2=1}^{\infty} \gamma_{j_1}^{-2}\; \gamma_{j_2}^{-2}\; H(\lambda_{j_1}, \lambda_f)\, H^*(\lambda_{j_2}, \lambda_f)$$

$$\times W_{\beta_1, j_1}(\xi_1)\, W^*_{\beta_2, j_2}(\xi_2)\, I(\mu_{j_1}, \lambda_{j_1}; \mu_{j_2}, \lambda_{j_2}; \omega) \tag{14}$$

$$\Phi_{MM}(\beta_1,\xi_1;\beta_2,\xi_2;\omega) = \left(\frac{B\,EI}{L}\right)^2 S_p(\omega) \sum_{j_1=1}^{\infty} \sum_{j_2=1}^{\infty} \gamma_{j_1}^{-2}\; \gamma_{j_2}^{-2}\, H(\lambda_{j_1}, \lambda_f)\, H^*(\lambda_{j_2}, \lambda_f)$$

$$\times W''_{\beta_1, j_1}(\xi_1)\, W^*_{\beta_2, j_2}{}''(\xi_2)\; I(\mu_{j_1}, \lambda_{j_1}; \mu_{j_2}, \lambda_{j_2}; \omega) \tag{15}$$

where the use has been made of $W_{\beta j}(\xi) = W^*_{\beta\, j}(\xi)$ due to its reality and the function $I(\cdot)$ is defined as

$$I(\mu_{j_1}, \lambda_{j_1}; \mu_{j_2}, \lambda_{j_2}; \omega) = \sum_{\beta_1'=1}^{N} \sum_{\beta_2'=1}^{N} \int_0^1 \int_0^1 \frac{\Phi_{pp}(\xi_1' - \xi_2' + \beta_1' - \beta_2'; \omega)}{S_p(\omega)}$$

$$\times W_{\beta_1', j_1}(\xi_1')\, W_{\beta_2', j_2}(\xi_2')\, d\xi_1'\, d\xi_2' \tag{16}$$

2.3 Derivation of Integral I(·)

Once the integral $I(\cdot)$ is determined, the cross-spectral densities of response are obtained by Eqs. (14) and (15). Taking into account the fact that the mode shape of N-span beam formulated in terms of the mode shapes of the infinite-span beam, see Eq. (12), and $\Phi_{pp}(\cdot)$ is real function, the expression for $I(\cdot)$ can be rewritten by

$$I(\mu_1, \lambda_1; \mu_2, \lambda_2; \omega) = \Lambda_1\, \Lambda_2\, [J(\mu_1, \lambda_1; \mu_2, \lambda_2; \omega) + \Gamma_1\, \Gamma_2\; J^*(\mu_1, \lambda_1; \mu_2, \lambda_2; \omega)$$

$$+ \Gamma_1\; J(-\mu_1, \lambda_1; \mu_2, \lambda_2; \omega) + \Gamma_2\; J^*(-\mu_1, \lambda_1; \mu_2, \lambda_2; \omega)] \tag{17}$$

where $J(\cdot)$ is given as

$$J(\mu_1, \lambda_1; \mu_2, \lambda_2; \omega) = \sum_{\beta_1'=1}^{N} \sum_{\beta_2'=1}^{N} R_{\beta_1', \beta_2'}$$

$$R_{\beta_1', \beta_2'} = \int_0^1 \int_0^1 \frac{\Phi_{pp}(\xi_1' - \xi_2' + \beta_1' - \beta_2'; \omega)}{S_p(\omega)}\; W_{\beta_1}(\xi_1', \mu_1, \lambda_1)\, W_{\beta_2}(\xi_2', \mu_2, \lambda_2)\, d\xi_1'\, d\xi_2' \tag{18}$$

Note that the span number β and the local coordinate ξ in mode shape $W_\beta(\cdot)$ can be separated. Thus the integration for $J(\cdot)$ can then be reduced to the combination of summations with respect to span number with a double integration in the local coordinate

system. The double summation in $J(\cdot)$ is separable into three sub-summations, symbolically indicated as follows

$$\sum_{\beta_1=1}^{N}\sum_{\beta_2=1}^{N} R_{\beta_1\beta_2} = \sum_{\beta_1}\sum_{>\beta_2} R_{\beta_1\beta_2} + \sum_{\beta_1}\sum_{<\beta_2} R_{\beta_1\beta_2} + \sum_{\beta_1}\sum_{=\beta_2} R_{\beta_1\beta_2} \tag{19}$$

The first two terms on the right side of Eq. (19) are evaluated to be

$$\sum_{\beta_1}\sum_{>\beta_2} R_{\beta_1\beta_2} = S_{NN}(A, \mu_1, \mu_2)\, K(A, \mu_1, \mu_2) + S_{NN}(A^*, \mu_1, \mu_2)\, K(A^*, \mu_1, \mu_2) \tag{20}$$

$$\sum_{\beta_1}\sum_{<\beta_2} R_{\beta_1\beta_2} = S_{NN}(A^*, \mu_2, \mu_1)\, K(A^*, \mu_2, \mu_1) + S_{NN}(A, \mu_2, \mu_1)\, K(A, \mu_2, \mu_1) \tag{21}$$

where

$$A = \alpha(\omega) + i\gamma(\omega) \tag{22}$$

and an asterisk indicates the complex conjugate. The function $S_{NN}(\cdot)$ reads

$$S_{NN}(A, \mu_1, \mu_2) = \sum_{\beta_2=1}^{N-1}\sum_{\beta_1=\beta_2+1}^{N} exp\,[-B_1(\beta_1 - 1) + B_2(\beta_2 - 1)]$$

$$= \begin{cases} \dfrac{e^{-B_1}(1 - e^{B_2}) + e^{(B_2-B_1)N}(1 - e^{-B_1}) - e^{-B_1 N}(1 - e^{B_2-B_1})}{(1 - e^{-B_1})(1 - e^{B_2})(1 - e^{B_2-B_1})}, & B_1 \neq B_2 \\ \dfrac{Ne^{-B} - e^{-BN} + 1 - N}{(1 - e^{-B})(1 - e^{B})}, & B_1 = B_2 = B \end{cases} \tag{23}$$

where

$$B_1 = A + i\mu_1;\ B_2 = A - i\mu_2 \tag{24}$$

and the function $K(\cdot)$ is defined as

$$K(A, \mu_1, \mu_2) = [a(\mu_1, \lambda_1)\ F(-A, \lambda_1) + b(\mu_1, \lambda_1) F(A, \lambda_1) e^{-A}]$$
$$\times [a(\mu_2, \lambda_2) F(A, \lambda_2) + b\ (\mu_2, \lambda_2) F(-A, \lambda_2) e^{A}] \tag{25}$$

where the coefficients of $a(\cdot)$ and $b(\cdot)$ are given in Appendix A and the function $F(\cdot)$ is obtained as

$$F(A, \lambda) = \int_0^1 e^{A\xi} f_\lambda(\xi)\, d\xi$$

$$= \frac{1}{2}\left\{ i\left[\frac{e^{A-i\lambda}-1}{A-i\lambda} - \frac{e^{A+i\lambda}-1}{A+i\lambda} \right] + \frac{sin\lambda}{sinh\lambda}\left[\frac{e^{A-\lambda}-1}{A-\lambda} - \frac{e^{A+\lambda}-1}{A+\lambda} \right] \right\} \tag{26}$$

The last term on the right side of Eq. (19) is derived as follows:

$$\sum_{\beta_1=\beta_2}\sum R_{\beta_1\beta_2} = \frac{1}{2} S_N(\mu_1+\mu_2)\,[K_0(A,\mu_1,\mu_2) + K_0(A^*,\mu_2,\mu_1)] \tag{27}$$

where $S_N(\mu_1 + \mu_2)$ is given by

$$S_N(\mu) = \sum_{\beta=1}^{N} e^{-i\mu(\beta-1)} = \begin{cases} \dfrac{1-e^{-i\mu N}}{1-e^{-i\mu}} & \mu \neq 2m\pi \\ N & \mu = 2m\pi \end{cases} \tag{28}$$

and the function $K_0(\cdot)$ is given by

$$K_0(A,\mu_1,\mu_2) = \int_0^1\int_0^1 exp\{-\alpha(\omega)\,|\xi_1-\xi_2| - i\gamma(\omega)(\xi_1-\xi_2)\}$$

$$\times W_1(\xi_1,\mu_1,\lambda_1)\,W_1(\xi_2,\mu_2,\lambda_2)\,d\xi_1 d\xi_2$$

$$= R(A,\mu_1,\mu_2) + R(A^*,\mu_2,\mu_1) \tag{29}$$

where

$$R(A,\mu_1,\mu_2) = \int_0^1 d\xi_1 \int_0^{\xi_1} d\xi_2\, exp\{-A(\xi_1-\xi_2)\}\, W_1(\xi_1,\mu_1,\lambda_1)\, W_1(\xi_2,\mu_2,\lambda_2)$$

$$= a_1 a_2 Q_{00}(A) + b_1 a_2 Q_{10}(A) + a_1 b_2 Q_{01}(A) + b_1 b_2 Q_{11}(A) \tag{30}$$

Here, $a_j = a(\mu_j, \lambda_j)$ and $b_j = b(\mu_j, \lambda_j)$ and the function Q is defined as

$$Q_{k_1,k_2}(A) = \int_0^1 d\xi_1 \int_0^{\xi_1} d\xi_2\; exp[-A(\xi_1-\xi_2)] f_{\lambda_1}(k_1-\xi_1) f_{\lambda_2}(k_2-\xi_2)$$

$$= T_{k_1,k_2}(A,\lambda_1,\lambda_2) + i\,\frac{sin\lambda_1}{sinh\lambda_1}\,T_{k_1,k_2}(A,i\lambda_1,\lambda_2)$$

$$+\; i\frac{sin\lambda_2}{sinh\lambda_2}\,T_{k_1,k_2}(A,\lambda_1,i\lambda_2) - \frac{sin\lambda_1\; sin\lambda_2}{sinh\lambda_1\; sinh\lambda_2}\,T_{k_1,k_2}(A,i\lambda_1,i\lambda_2) \tag{31}$$

where the function $T(\cdot)$ is given as

$$T_{k_1,k_2}(A, \lambda_1, \lambda_2) = \int_0^1 d\xi_1 \int_0^{\xi_1} d\xi_2 \, e^{-A\xi_1 + A\xi_2} \sin\lambda_1 (k_1 - \xi_1) \sin\lambda_2 (k_2 - \xi_2)$$

$$= U(A, \lambda_1, \lambda_2) + U(A, -\lambda_1, -\lambda_2) \tag{32}$$

with

$$U(A, \lambda_1, \lambda_2) = \frac{e^{i\lambda_2 k_2}}{4(A - i\lambda_2)} \left\{ e^{-i\lambda_1 k_1} \left[\frac{e^{i(\lambda_1 - \lambda_2)} - 1}{i(\lambda_1 - \lambda_2)} (1 - \delta_{\lambda_1\lambda_2}) + \delta_{\lambda_1\lambda_2} + \frac{e^{-(A - i\lambda_1)} - 1}{A - i\lambda_1} \right] \right.$$

$$\left. + e^{i\lambda_1 k_2} \left[\frac{e^{-i(\lambda_1 + \lambda_2)} - 1}{i(\lambda_1 + \lambda_2)} - \frac{e^{-(A + i\lambda_1)} - 1}{A + i\lambda_1} \right] \right\} \tag{33}$$

where δ is the Kronecker's delta.

2.4. Numerical Results

Once the integral of $I(\cdot)$ defined in Eq. (16) is determined, then the cross-spectral density of response for both the displacement Φ_{DD} and the bending moment Φ_{MM} can be obtained by Eqs. (14) and (15), respectively. The covariance functions of displacement and bending moment can be directly obtained by integrating the cross-spectral density with respect to ω, i.e.

$$R_{ww}(x_1, x_2) = \int_{-\infty}^{+\infty} \Phi_{DD}(x_1, x_2; \omega) \, d\omega$$

$$R_{MM}(x_1, x_2) = \int_{-\infty}^{+\infty} \Phi_{MM}(x_1, x_2; \omega) \, d\omega \tag{34}$$

When $x_1 = x_2 = x$, the mean-square values of responses at x are obtained from above Eq. (34).

Three numerical examples, namely two-, four- and six-span beam were selected. All the three beams were taken to have the same material properties; beam's width $B = 1.1$ (in); bending stiffness $EI = 7.41 \times 10^5$ ($lb_f in^2$), $\rho A = 0.0747$ (lb_m/in); span length $L = 53.28$ (in). Figs. 1(a), 1(b) and 1(c) portray the spectral density of displacement at mid-point of second span for various multi-span beams. It is seen that the number of peaks in the first propagation band equals to the number of spans. The peaks can only occur in each frequency passing band. The numerical results show that the effects of the mode shapes

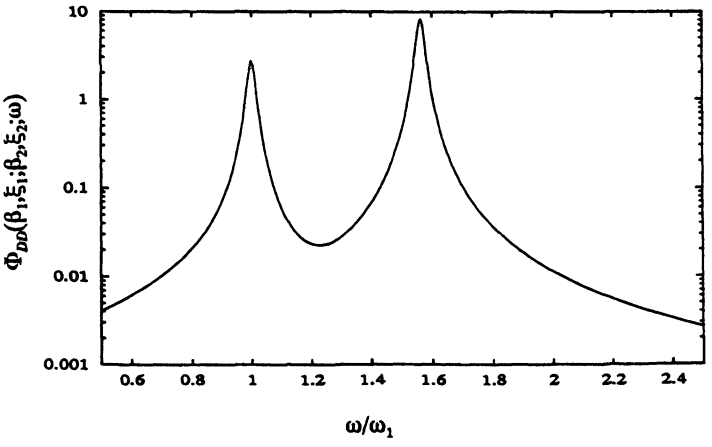

Figure 1 (a). Spectral density of displacement for a two-span beam ($\beta_1 = \beta_2 = 2$; $\xi_1 = \xi_2 = 0.5$).

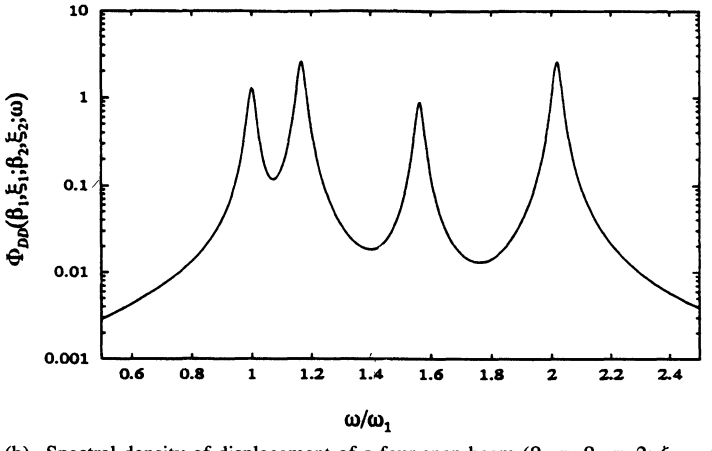

Figure 1 (b). Spectral density of displacement of a four-span beam ($\beta_1 = \beta_2 = 2$; $\xi_1 = \xi_2 = 0.5$).

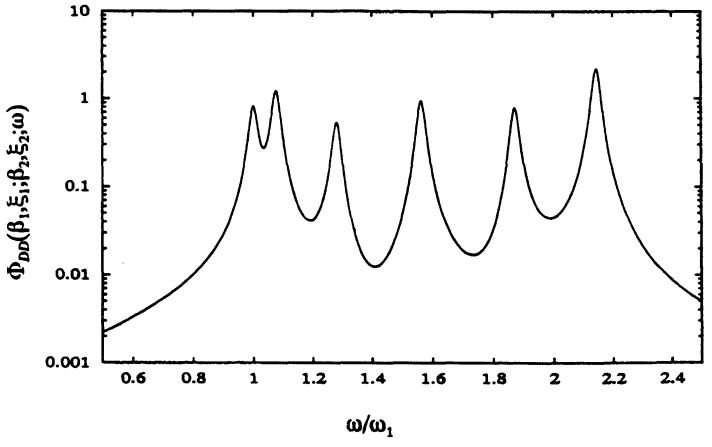

Figure 1 (c). Spectral density of displacement for a six-span beam ($\beta_1 = \beta_2 = 2$; $\xi_1 = \xi_2 = 0.5$).

associated with the higher frequency-passing band are negligible for the cross-spectral densities of response at the low frequencies.

3. CONVEX MODELING OF ACOUSTIC LOADING AND ITS APPLICATION

The model of cross-spectral density for acoustic loading in the launch site is composed of three functions, namely spectral density $S_p(\omega)$, decay function $\alpha(\omega)$, and phase function $\gamma(\omega)$ which best fit the measurements (see Appendix B). However, these three functions exhibit uncertainties due to the scatter of the measurement data. This uncertainty in the functions can be characterized by a set of uncertain parameters, namely u_1, u_2, and u_3 in above functions. These parameters are assumed to belong to a bounded, convex set. To find such a convex set, the ellipsoidal set, let us first establish a minimum-volume three-dimensional box (Fig. 2(a))

$$| u_i | \leq e_i, \ (i = 1, 2,, 3) \tag{35}$$

to which the data belong. Then we enclose this box by an ellipsoid

$$\frac{u_1^2}{g_1^2} + \frac{u_2^2}{g_2^2} + \frac{u_3^2}{g_3^2} \leq 1 \tag{36}$$

where g_i are the semi-axes of the ellipsoid (Fig. 2(b)). There are infinite number of ellipsoids which contain the box Eq. (35). Clearly, the best choice is the one with the minimum volume. The volume of a three-dimensional ellipsoid is given by

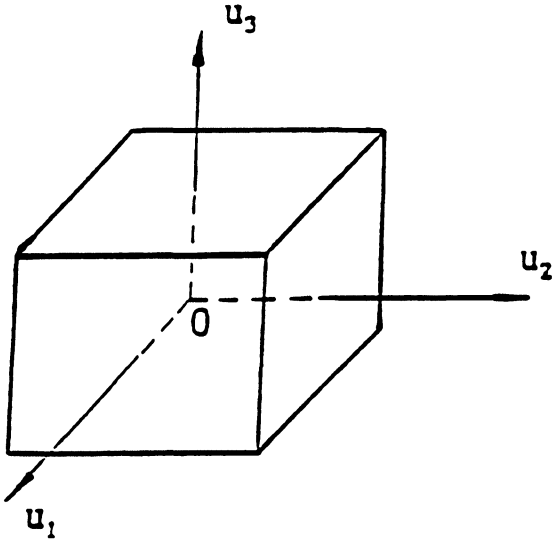

Figure 2 (a). Uncertainty box.

$$V = \frac{4}{3}\pi g_1 g_2 g_3 \tag{37}$$

The surface of the ellipsoid should pass through the corner points of the box (35). Therefore,

$$\frac{e_1^2}{g_1^2} + \frac{e_2^2}{g_2^2} + \frac{e_3^2}{g_3^2} = 1 \tag{38}$$

We are interested in minimizing the volume V of the ellipsoid, subject to constraint (38). By using the Lagrange multiplier technique. The Lagrangian reads

$$E = \frac{4}{3}\pi g_1 g_2 g_3 + \lambda\left(\frac{e_1^2}{g_1^2} + \frac{e_2^2}{g_2^2} + \frac{e_3^2}{g_3^2} - 1\right) \tag{39}$$

By requiring

$$\frac{\partial E}{\partial g_i} = 0, \ (i = 1, 2, 3) \tag{40}$$

One obtains

$$\frac{4}{3}\pi g_2 g_3 - \frac{2\lambda e_1^2}{g_1^3} = 0 \tag{41}$$

$$\frac{4}{3}\pi g_1 g_3 - \frac{2\lambda e_2^2}{g_2^3} = 0 \tag{42}$$

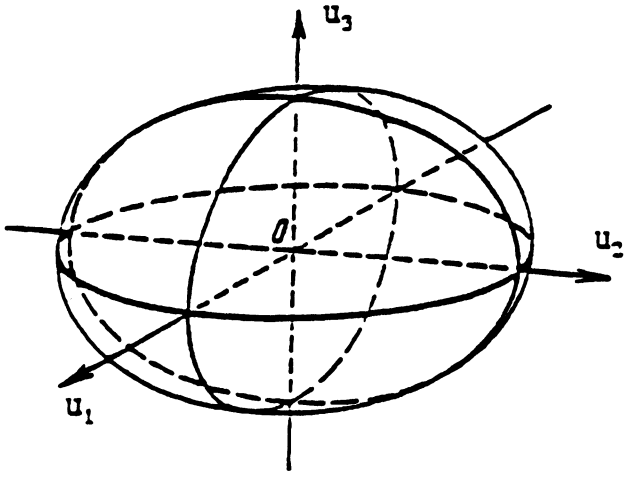

Figure 2 (b). Uncertainty ellipsoid.

$$\frac{4}{3}\pi g_1 g_2 - \frac{2\lambda e_3^2}{g_3^3} = 0 \tag{43}$$

Multiplying Eq.(41) by g_1, Eq.(42) by g_2, Eq.(43) by g_3, and summing up the results, we obtain

$$3V - 2\lambda\left(\frac{e_1^2}{g_1^2} + \frac{e_2^2}{g_2^2} + \frac{e_3^2}{g_3^2}\right) = 0 \tag{44}$$

Combining Eqs.(38) and (44), we have

$$\lambda = \frac{3}{2} V \tag{45}$$

Substitution of Eq.(45) into Eq.(41) results in

$$\frac{V}{g_1} - 3\frac{e_1^2}{g_1^3} V = 0 \tag{46}$$

Since V is non-zero, we get

$$g_1 = \sqrt{3}\, e_1 \tag{47}$$

In full analogy

$$g_2 = \sqrt{3}\, e_2, \quad g_3 = \sqrt{3}\, e_3 \tag{48}$$

Thus, once the size of the box (35) is known, the semi-axes of the minimum-volume ellipsoid enclosing the box of the experimental data is readily determined utilizing Eqs. (47) and (48). The results can be extended to a more general N-dimensional case. Assume the size of this N-dimensional box is given

$$|u_i| \leq e_i, \ (i = 1, 2, \ldots, N) \tag{49}$$

By using the same procedure, the semi-axes of the minimum-volume ellipsoid enclosing the given N-dimensional box can be obtained as

$$g_i = \sqrt{N}\, e_i, \ (i = 1,2, \ldots, , N) \tag{50}$$

Figures 3, 4(a)–4(c), and 5(a)–5(c) portray the fitted statistical characteristics of the acoustic excitation using the recorded data. Figure 3 is obtained for the spectral density, Figures 4(a)–4(c) for the coherence function, and Figures 5(a)–5(c) for the phase function.

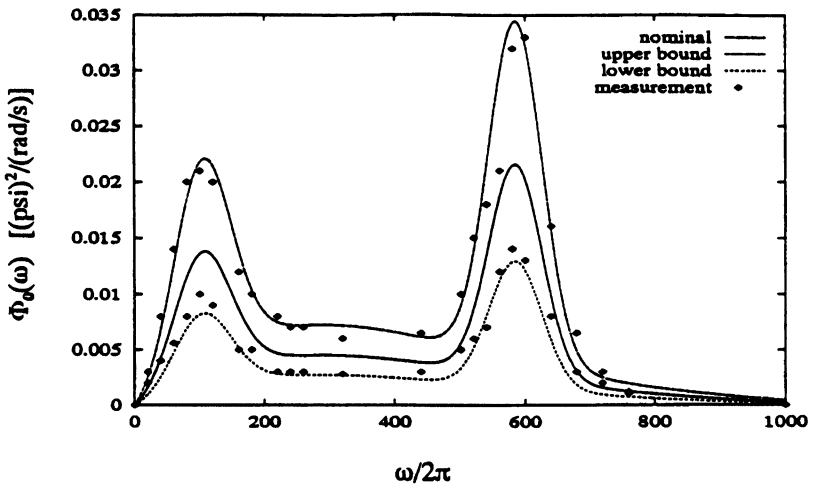

Figure 3. Spectral density of excitation.

The half lengths of the sides of the uncertainty box given by (B.5) are

$$e_1 = 0.5, \quad e_2 = 0.3, \quad e_3 = 1. \tag{51}$$

Note that Eqs. (B1), (B2), and (B3), modeling the statistical characteristics of the loading, have been constructed in such a manner that the nominal values u_j^0 are zero.

In Figure 3 the Curve 1 is associated with the nominal value $u_1^0 = 0$, curve 2 with the maximum value $u_1^+ = 0.5$, and curve 3 associated with the minimum value $u_1^- = -0.5$. Analogously, Figures 4(a)–4(c) portray the coherence function at a spatial separation distances, namely x_1–$x_2 = 10.4$ ft, x_1–$x_2 = 20.75$ ft and x_1–$x_2 = 31.17$ ft, along with the upper (curve 2) and lower (curve 3) envelopes. Curve 1 is associated with the nominal value $u_2^0 = 0$. Figures 5(a)–5(c) portray, respectively, the phase coefficient function at the same three separation distances.

In Figures 4(a)–4(c) and 5(a)–5(c) some representative experimental data are also included. They are indicated by small squares. Numerical calculations have been carried out for a single-span beam and a ten-span beams, both of which are simply supported at the ends. The two beams have the same flexural stiffness $EI = 7.41 \times 10^5$ ($lb_f.in^2$), mass per unit length $\rho A = 0.0747$(lb/in), width $B = 1.1$(in), and individual span length $L = 53.28$(in).

The analysis for single-span and multi-span beams proceeds in exactly the same manner as the case of the single-degree-of-freedom system investigated by Elishakoff and Colombi [16]. Here, as in [16] it is postulated that the uncertain parameters, u_1, u_2 and u_3 belong to the ellipsoid

$$\{\delta\}^T [\Omega] \{\delta\} \leq 1 \tag{52}$$

where

$$\{\delta\}^T = (u_1, u_2, u_3) \tag{53}$$

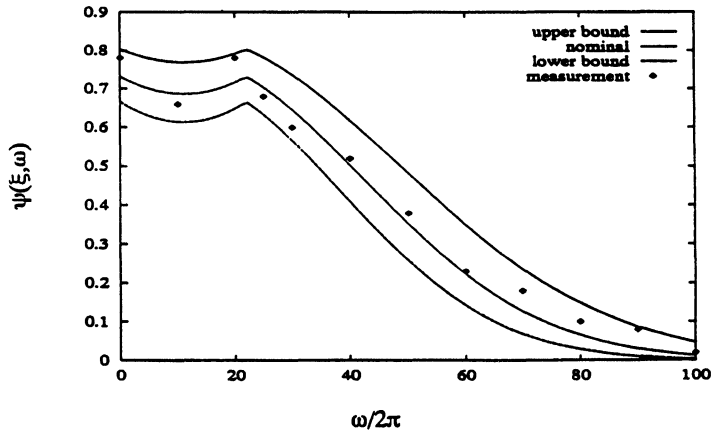

Figure 4 (a). Coherence function $\psi(\xi,\omega) = e^{-\alpha(\infty)|\xi|}$ at separation distance $\xi = 10.4$ ft.

and Ω is a positive-definite symmetric matrix which provides an information on the size as well as the shape of the ellipsoid. The matrix Ω, for example, in Eq. (52) becomes, after the fit is performed to the experimental data:

$$\Omega = \begin{bmatrix} \frac{4}{3} & 0 & 0 \\ 0 & \frac{100}{27} & 0 \\ 0 & 0 & \frac{1}{3} \end{bmatrix} \tag{54}$$

with $\Omega_{jj} = g_j^{-2}$, where g_j's are defined in Eqs. (47) and (48). In addition, vector grad $\bar{f}$ contains three elements

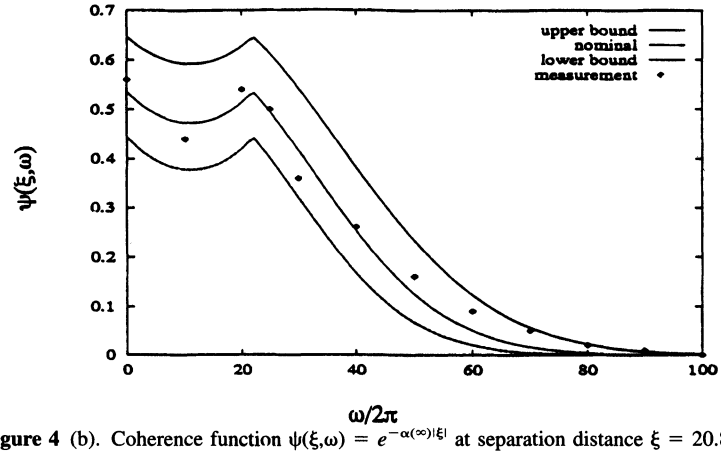

Figure 4 (b). Coherence function $\psi(\xi,\omega) = e^{-\alpha(\infty)|\xi|}$ at separation distance $\xi = 20.8$ ft.

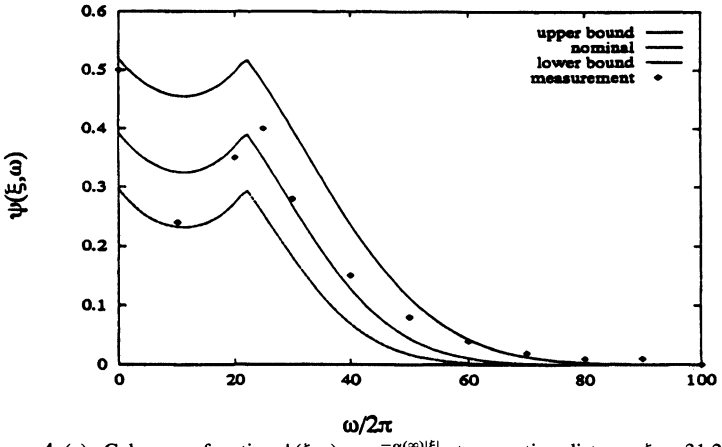

Figure 4 (c). Coherence function $\psi(\xi,\omega) = e^{-\alpha(\infty)|\xi|}$ at separation distance $\xi = 31.2$ ft.

$$grad\,\{\bar{f}(u_1, u_2, u_3)\} = \left[\frac{\partial \bar{f}}{\partial u_1}, \frac{\partial \bar{f}}{\partial u_2}, \frac{\partial \bar{f}}{\partial u_3}\right] \tag{55}$$

where $\bar{f}$ is defined as

$$\bar{f}(u_1, u_2, u_3) = \frac{E\,[w^2(u_1, u_2, u_3)]}{E\,[w^2(u_1^0, u_2^0, u_3^0)]} \tag{56}$$

where the mean-square values of response for the multi-span beams can be evaluated by Eq. (34) in previous section, which are also the function of the uncertain parameters u_i. The expressions both for the maximum and minimum responses read [16]:

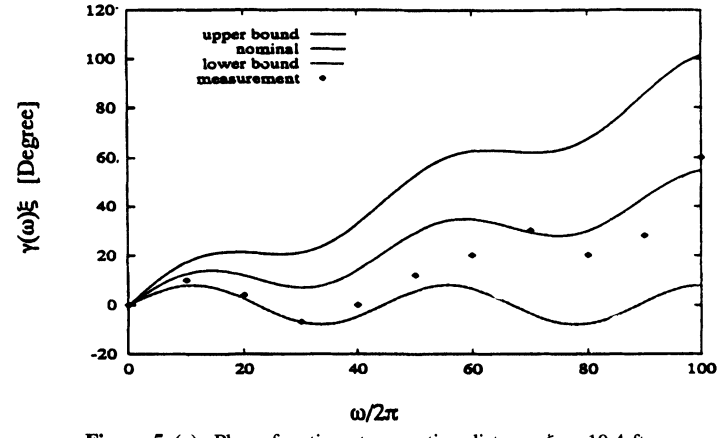

Figure 5 (a). Phase function at separation distance $\xi = 10.4$ ft.

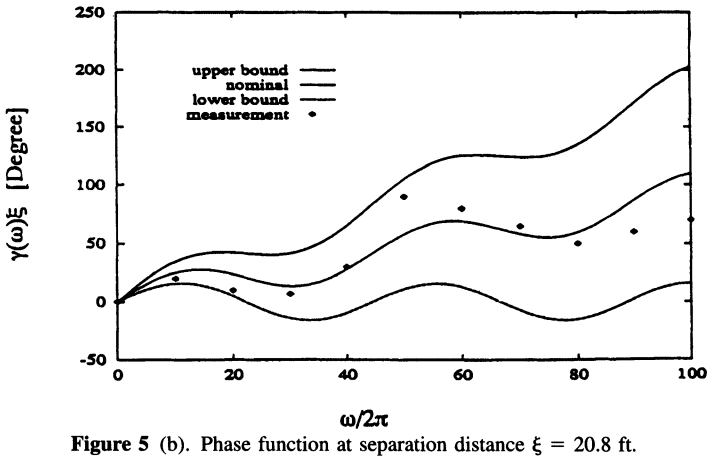

Figure 5 (b). Phase function at separation distance $\xi = 20.8$ ft.

$$E[w^2(u_1, u_2, u_3)]_{max} = E[w^2(u_1^0, u_2^0, u_3^0)]\{1 + \sqrt{(grad f)_0^T \Omega^{-1} (grad f)_0}\}$$

$$E[w^2(u_1, u_2, u_3)]_{min} = E[w^2(u_1^0, u_2^0, u_3^0)]\{1 - \sqrt{(grad f)_0^T \Omega^{-1} (grad f)_0}\} \quad (57)$$

where u_1^0, u_2^0 and u_3^0 are the nominal values of the uncertain parameters u_1, u_2, and u_3, respectively, and the subscript 0 means that the derivatives are evaluated at the nominal values, u_i^0 $(i = 1, 2, 3)$.

The least favorable responses may be evaluated either by utilizing an uncertainty box or an uncertainty ellipsoid. When the uncertain parameters are confined to an uncertainty box, the response must be calculated at the center of the box, yielding the nominal response, as well as the four corners, the twelve mid-points of the sides, and the six mid-points on the surface planes of the box, and inside the box. For the single-span beam, the results are obtained as follows [17]:

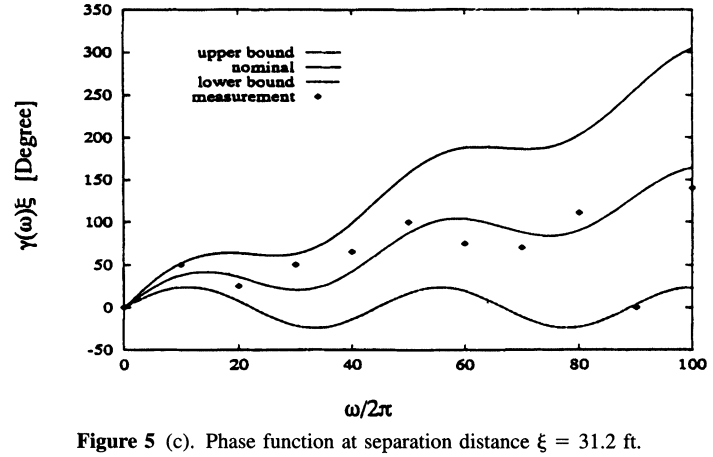

Figure 5 (c). Phase function at separation distance $\xi = 31.2$ ft.

$$E\,[w_1^2\,(0.5)]_{max} = 0.131\ (in^2)$$

$$E\,[w_1^2\,(0.5)]_0 = 0.086\ (in^2)$$

$$E\,[w_1^2\,(0.5)]_{min} = 0.043\ (in^2) \tag{58}$$

It is remarkable that the least favorable mean-square displacement. $E\,[w^2]_{\max}$ occurs at the following values of uncertain parameters u_j:

$$u_1 = 0.5, \quad u_2 = -0.3, \quad u_3 = -1 \tag{59}$$

In other words the maximum response does not necessarily correspond to the maximum values of the uncertain parameters which could be the case with monotonically increasing function. The mean-square value of the response $E\,[w^2]$ obtained with $u_1 = 0.5$, $u_2 = 0.3$ and $u_3 = 1$ is 0.12 in^2, which is 2.44% lower than the maximum value 0.131 in^2 in Eq. (58). For the ten-span beams at the mid-point of the first span beam, the results are

$$E\,[w_1^2\,(0.5)]_{max} = 0.247\ in^2$$

$$E\,[w_1^2\,(0.5)]_0 = 0.147\ in^2$$

$$E\,[w_1^2\,(0.5)]_{min} = 0.064\ in^2 \tag{60}$$

In this case, the maximum response is obtained when the uncertain parameters u_j take on their maximum values.

Calculation using formula Eq. (57) for the uncertainty ellipsoid yields, for the single-span beam

$$E\,[w_1^2\,(0.5)]_{max} = 0.161\ in^2$$

$$E\,[w_1^2\,(0.5)]_{min} = 0.011\ in^2 \tag{61}$$

Maximum response occurs at the following values of uncertainty parameters

$$u_1 = 0.866, \quad u_2 = -0.011, \quad u_3 = 0. \tag{62}$$

For the ten-span beams, the ellipsoidal modeling of excitation yields

$$E\,[w_1^2\,(0.5)]_{max} = 0.277\ in^2$$

$$E\,[w_1^2\,(0.5)]_{min} = 0.016\ in^2 \tag{63}$$

with the maximum response occurring at

$$u_1 = 0.147, \quad u_2 = -0.058, \quad u_3 = -0.030 \tag{64}$$

For the single-span beam the gradient of the response reads

$$(grad\bar{f})_0^T = [0.086, -0.003, 0] \tag{65}$$

This implies that the variation of the uncertain parameters u_3 does not contribute to the response variability. Analogous conclusion holds also for the ten-span beams, for which

$$(grad\bar{f})_0^T = [0.147, 0.058, 0.001] \tag{66}$$

The maximum value predicted by the ellipsoidal model of uncertainty is about 23% higher than the value predicted by the uncertainty box, for the single-span beam. This can be explained by the fact that the uncertainty ellipsoid contains the uncertainty box. For the ten-span beams the least favorable response obtained from the ellipsoidal modeling exceeds its counterpart from the uncertainty box by about 12%. Some conservatism, associated with the ellipsoidal modeling, is justified since the ellipsoidal modeling is computational very inexpensive.

ACKNOWLEDGMENT

This study has been supported by the NSF through the grants MSM-9215698 (Program Director: Dr. K. P. Chong). This support is gratefully appreciated. Any opinions, findings or recommendations expressed by this publication are those of the authors and do not necessarily reflect the views of the NSF. We also are grateful to Elsevier Science Publishers for permission to draw some parts of Ref. 17.

References

1. H. Abramovich and I. Elishakoff, Application of the Krein's Method for Determination of Natural Frequencies of Periodically Supported Beam Based on Simplified Bresse-Timoshenko Equations, *Acta Mechanica* **66** (1987), 39–59.
2. M. G. Krein, Vibration Theory of Multi-Span Beams, *Vestnik Inzhenerov i Tekhnikov* **4** (1933), 142–145 (in Russian).
3. Y. K. Lin, Free Vibration of a Continuous Beam on Elastic Supports, *International Journal of Mechanical Sciences* **4** (1962), 409–423.
4. J. W. Miles, Vibration of Beams on Many Supports, *Journal of Engineering Mechanics* **82** (1956), 1–9.
5. G. Sen Gupta, Natural Flexural Wave and the Normal Modes of Periodically-Supported Beams and Plates, *Journal of Sound and Vibration* **13** (1970), 89–101.
6. Y. K. Lin and T. J. McDaniel, Dynamics of Beam Type Periodic Structures, *Journal of Engineering for Industry* **93** (1969), 1133–1141.
7. Y. K. Lin, S. Maekawa, H. Nijim, and L. Maestrello, Response of Periodic Beam to Supersonic Boundary-Layer Pressure Fluctuations, in *Stochastic Problems in Dynamics* B. L. Clarkson, (Ed.), Pitman, 1977, pp. 468–485.
8. D. J. Mead, Free Wave Propagation in Periodically-Supported Infinite Beams, *Journal of Sound and Vibration* **11** (1970), 181–197.
9. D. J. Mead, Space-Harmonic Analysis of Periodically Supported Beams: Response to Convected Random Loading, *Journal of Sound and Vibration* **14** (1971), 525–541.
10. D. Li and H. Benaroya, Dynamics of Periodic and Near-Periodic Struvtures, *Applied Mechanics Reviews* **45** (1992), 447–460.
11. S. T. Ariaratnam and W. C. Xie, On the Localization Phenomenon in Randomly Disordered Engineering Structures, in *Nonlinear Stochastic Mechanics* N. Bellomo and F. Casciati, (Eds.), Springer New York, 1992, pp. 13–24.

12. C. H. Hodges and J. Woodhouse, Vibration Isolation from Irregularity in a Nearly Periodic Structure: Theory and Measurements, *Journal of Acoustical Society of America* **74** (1983), 894–905.
13. C. Pierre and E. H. Dowell, Localization of Vibrations due to Structural Irregularity, *Journal of Sound and Vibration* **114** (1987), 549–564.
14. I. Elishakoff, Y. W. Li, and J. H. Starnes, Jr., Buckling Mode Localization in Elastic Plates Due to Misplacements in the Stiffener Location, *An Interdisciplinary Journal of Nonlinear Scienee: Chaos, Solitons and Fractals* **5** (1995), to appear.
15. L. P. Zhu, I. Elishakoff, and Y. K. Lin, Free and Forced Vibrations of Periodic Multi-Span Beams, *Journal of Shock and Vibration* **1** (1994), 217–232.
16. I. Elishakoff and P. Colombi, Combination of Probabilitic and Convex Models of Uncertainty When Scarce Knowledge Is Present on Acoustic Excitation Parameters, *Computer Methods in Applied Mechanics and Engineering* **104** (1993), 187–209.
17. I. Elishakoff, Y. K. Lin and L. P. Zhu, *Probabilistic and Convex Modeling of Acoustically Excited Structures*, Elsevier, Amsterdam, 1994.

APPENDIX A

The mode shapes of multi-span beam were obtained in [10]. For an infinite-span beam, the deflection functions may be written as follows:

$$W_\beta[\xi,\mu,\lambda] = [a(\mu,\lambda)f_\lambda(\xi) + b(\mu,\lambda)f_\lambda(1-\xi)]e^{-i\mu(\beta-1)},$$
$$(\beta = 0,\pm1,\pm2,\cdots,\pm\infty) \tag{A.1}$$

where subscript β is the serial number of span. $f_\lambda(\cdot)$, $a(\cdot)$ and $b(\cdot)$ are, respectively, defined as

$$f_\lambda(\xi) = sin\lambda\xi - \frac{sin\lambda}{sinh\lambda} sinh\lambda\xi \tag{A.2}$$

$$a(\mu,\lambda) = \begin{cases} f_\lambda'(1)e^{-i\mu} - f_\lambda'(0), & \mu \neq m\pi \\ 1, & \mu = m\pi \end{cases} \tag{A.3}$$

$$b(\mu,\lambda) = \begin{cases} f_\lambda'(0)e^{-i\mu} - f_\lambda'(1), & \mu \neq m\pi \\ (-1)^{s+1}, & \mu = m\pi \end{cases} \tag{A.4}$$

Here, s = the integer of $[\lambda/\pi]$ coincides the number of propagation band in which λ is located.

For a finitely long multi-span beam, the angular displacement function Θ_β may be expressed in terms of complex form as

$$\Theta_\beta = \Lambda_j(e^{i\mu_j\beta} + \Gamma_j e^{-i\mu_j\beta}) \tag{A.5}$$

Hence, the mode shape can be expressed in terms of that of infinitely long multi-span beam as follows:

$$W_{\beta_j}(\xi) = \Lambda_j[W_\beta(\xi,\mu_j,\lambda_j) + \Gamma_j W_\beta(\xi,\mu_j,\lambda_j)],$$
$$(\beta = 1,2,\cdot\ \cdot\ \cdot,N) \tag{A.6}$$

where the coefficients Λ_j and Γ_j are defined as

$$\Lambda_j = \frac{1}{2};\ \Gamma_j = 1, \quad \text{for} \quad \mu_j = m\pi \quad \text{or} \quad \Theta_\beta = cos\mu_j\beta;$$

$$\Lambda_j = \frac{1}{2i};\ \Gamma_j = -1, \quad \text{for} \quad \Theta_\beta = sin\mu_j\beta \quad \text{and} \quad \mu_j \neq m\pi. \tag{A.7}$$

The wave constant μ and angular displacement function Θ_β with various boundary conditions at the ends of beam structures are listed in following Table I:

APPENDIX B

The model of cross-spectral density for acoustic loading is given by Eq. (2), in which the three parameter functions, namely spectral density $S_p(\omega)$, decay function $\alpha(\omega)$, and phase function $\gamma(\omega)$ are introduced to fit best the experiment data. The spectral density is approximated analytically as follows

$$S_p(\omega) = (1 + u_1)\sum_{i=1}^{3} a_i\left(\frac{\omega}{\omega_i}\right)\exp\left(-\frac{D_i}{2(1-c_i)}\right)$$
$$D_i = \left(\frac{\omega}{\omega_i} - c_i\right)^2 - (1-c_i)^2,\ \omega_i = 2\pi b_i \tag{B.1}$$

where the parameters a_i, b_i and c_i are listed in Table II.

TABLE I. Angular Displacement and Wave Constant of N-Span Beam with Various Boundary Conditions

Boundary Conditions	Θ_β ($\mu \neq m\pi$)	Equation for μ	$\frac{\mu_{(s-1)N+r}}{\pi}$
Simple–Simple	$\cos\mu\beta$	$\sin\mu = 0$	$\frac{1}{2}[1 - (-1)^s] + (-1)^s\frac{r-1}{N}$
Clamped–Clamped	$\sin\mu\beta$	$\sin\mu = 0$	$\frac{1}{2}[1 - (-1)^s] + (-1)^s\frac{r}{N}$
Simple–Clamped	$\cos\mu\beta$	$\cos\mu = 0$	$\frac{1}{2}[1 - (-1)^s] + (-1)^s\frac{2r-1}{2N}$
Clamped–Simple	$\sin\mu\beta$	$\cos\mu = 0$	$\frac{1}{2}[1 - (-1)^s] + (-1)^s\frac{2r-1}{2N}$

Table II. Parameters Decribing the Spectral density $S_p(\omega)$

i	1	2	3
a_i [(psi)^2/(r/s)]	$1.1\text{x}10^{-2}$	$4.5\text{x}10^{-3}$	$1.9\text{x}10^{-2}$
b_i[Hz]	105	290	585
c_i	0.8	-1.0	0.995

The decay formula is modeled as

$$\alpha(\omega) = (1 + u_2)\,(0.03 + 5.10^{-5}\,\frac{\omega}{2\pi}\,|\,\frac{\omega}{2\pi} - 22\,|\,) \tag{B.2}$$

and has a dimension ft^{-1}. The phase function is defined as

$$\gamma(\omega) = 0.77 \sin\left(0.14\,\frac{\omega}{2\pi}\right) + 0.045\,(1 + u_3)\,\frac{\omega}{2\pi} \tag{B.3}$$

and has a dimension of degree/ft. The uncertain parameters u_i (i = 1,2,3) in Eqs (B.1), (B.2) and (B.3) are assumed to vary in a box

$$|\,u_i\,| \leq e_i,\ (i = 1,2,3) \tag{B.4}$$

The bounds of the box are

$$e_1 = 0.5, \quad e_2 = 0.3, \quad e_3 = 1 \tag{B.5}$$

when $u_i = 0$ correspond to the nominal values of three coefficient functions.